Carbohydrate Polymers 74 (2008) 552–558

Contents lists available at ScienceDirect

Carbohydrate Polymers

journal homepage: www.elsevier.com/locate/carbpol

# Effects of plasticizers on the structure and properties of starch–clay nanocomposite films

Xiaozhi Tang [a], Sajid Alavi [b,*], Thomas J. Herald [a]

[a] Food Science Institute, Kansas State University, Manhattan, KS 66506, USA
[b] Department of Grain Science & Industry, Kansas State University, Manhattan, KS 66506, USA

ARTICLE INFO

*Article history:*
Received 28 October 2007
Received in revised form 29 February 2008
Accepted 7 April 2008
Available online 22 April 2008

*Keywords:*
Plasticizer
Starch
Clay
Nanocomposite
Film

ABSTRACT

Biodegradable nanocomposites were successfully fabricated from corn starch and montmorillonite (MMT) nanoclays by melt extrusion processing. The structure and morphology of the nanocomposites were characterized by X-ray diffraction (XRD) and transmission electron microscopy (TEM), and film properties such as barrier, mechanical and thermal properties were also measured. As a conventional plasticizer, the influence of glycerol content was first investigated. As the glycerol content decreased from 20% to 5%, the degree of clay exfoliation increased. Films with 5% glycerol exhibited the lowest water vapor permeability (0.41 g mm/kPa h $m^2$), highest glass transition temperature (53.78 °C), and highest tensile strength (35 MPa), but low elongation at break (2.15%). Urea and formamide were tested as alternative plasticizers for the starch–clay nanocomposites. The results indicated that the use of new plasticizers increased the degree of clay exfoliation. The formamide plasticized starch–clay nanocomposite films exhibited lower water vapor permeability (0.58 g mm/kPa h $m^2$), higher glass transition temperature (54.74 °C), and higher tensile strength (26.64 MPa) than the other two plasticizers when used at the same level (15 wt%).



## 1. Introduction

Polymer-layered silicate (PLS) nancomposites have been the focus of academic and industrial attention in recent years because the final composites often exhibit a desired enhancement of mechanical, barrier, thermal, and/or other properties relative to the original polymer matrix, even at very low clay contents (Giannelis, 1996; Ray, Quck, Easteal, & Chen, 2006; Sinha Ray & Okamoto, 2003; Sorrentino, Gorrasi, & Vittoria, 2007). In addition, the silicate clays used in such nanocomposites are environmentally friendly, naturally abundant, and economical. Normally, natural or organically modified clay, which in the pure state has a stacked structure of parallel silicate layers, is put in direct contact with the polymer matrix or its precursor monomers and the nanocomposites are subsequently obtained by one of several methods, including in situ polymerization, intercalation from solution, or melt intercalation (Sinha Ray & Okamoto, 2003). For real nanocomposites, the clay layers must be uniformly dispersed in the polymer matrix (intercalated or exfoliated), as opposed to being aggregated as tactoids (Fig. 1). A diverse array of matrix polymers have been used in PLS nanocomposite formation, ranging from synthetic non-degradable polymers such as nylon (Dennis et al., 2001; Kojima et al., 1993a; Kojima et al., 1993b), polystyrene (Vaia & Giannelis, 1997; Vaia, Jandt, Kramer, & Giannelis, 1995), and polypropylene (Kurokawa, Yasuda, & Oya, 1996; Usuki, Kato, Okada, & Kurauchi, 1997) to biopolymers such as polylactide (Sinha Ray, Maiti, Okamoto, Yamada, & Ueda, 2002; Sinha Ray, Yamada, Okamoto, & Ueda, 2002) and starch (Avella et al., 2005; De Carvalho, Curvelo, & Agnelli, 2001; Pandey & Singh, 2005; Park, Lee, Park, Cho, & Ha, 2003; Park et al., 2002; Wilhelm, Sierakowski, Souza, & Wypych, 2003; Chiou et al., 2007).

Starch is attractive because it is a cheap material and has very fast biodegradation rate. Under high temperature and shear, starch can be processed into a moldable thermoplastic, known as thermoplastic starch (TPS). During the thermoplastic process, water contained in starch and the added plasticizers play an indispensable role because the plasticizers can form hydrogen bonds with the starch, replacing the strong interactions between the hydroxyl groups of the starch molecules, and thus making starch thermoplastic (Hulleman, Janssen, & Feil, 1998; Ma & Yu, 2004; Ma, Yu, & Feng, 2004).

In a previous study (Tang, Alavi, & Herald, 2008), we fabricated starch–clay nanocomposites by extrusion processing using glycerol as the plasticizer. The results indicated that the interactions between the starch matrix and clay surface were crucial to the formation of nanostructure. Because the plasticizers play an indispensable role in the starch thermoplastic process due to the interactions between starch and plasticizers, it was hypothesized that plasticizers might also participate in the interactions between

* Corresponding author. Tel.: +1 785 532 2403; fax: +1 785 532 4017.
*E-mail address:* salavi@ksu.edu (S. Alavi).

0144-8617/$ - see front matter © 2008 Elsevier Ltd. All rights reserved.
doi:10.1016/j.carbpol.2008.04.022

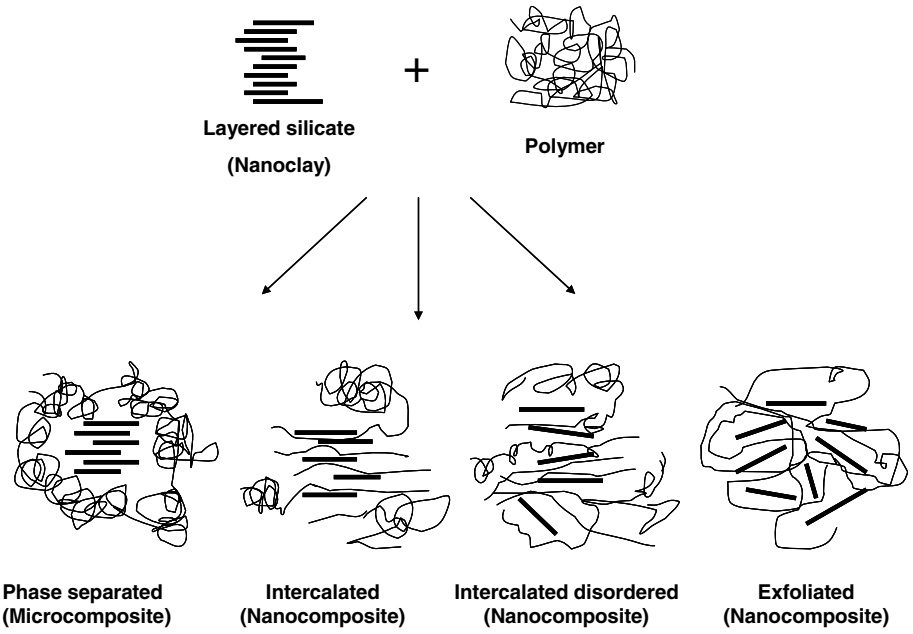


**Fig. 1.** Schematic representation of intercalated and exfoliated nanocomposite from layered silicate clay and polymer.

starch and clay and therefore could greatly affect the formation of nanostructure and further influence the mechanical and water vapor barrier properties of starch–clay nanocomposite films.

In the present study, we tested the influence of glycerol content and different plasticizers (glycerol, urea, and formamide) on the formation of nanostructure and properties of the starch–clay nanocomposite films.

## 2. Materials and methods

### 2.1. Materials

Regular cornstarch was obtained from Cargill Inc. (Cedar Rapids, IA). Montmorillonite (MMT) nanoclay was obtained from Nanocor Inc. (Arlington Heights, IL). Glycerol, urea, and formamide were obtained from Sigma (St. Louis, MO).

### 2.2. Preparation of plasticized starch–clay nanocomposites

Glycerol (0–20 wt%), urea (15 wt%), and formamide (15 wt%) were used to plasticize the starch/clay nanocomposite system. The nanocomposite preparation was performed using a lab-scale twin-screw extruder (Micro-18, American Leistritz, Somerville, NJ) with a six-head configuration and screw diameter of 18 mm and L/D ratio of 30:1. The screw configuration and barrel temperature profile (85–90–95–100–110–120 °C from feed zone to die) are shown in Fig. 2. Dry starch, plasticizers, clay (6 wt%), and water (19 wt%) mixtures were extruded at a screw speed of 200 RPM. The extrudates were ground using a Wiley mill (model 4, Thomas-Wiley Co., Philadelphia, PA) and an Ultra mill (Kitchen Resource LLC, North Salt City, UT) for further use.

### 2.3. Structural characterization of starch–nanoclay composites

X-ray diffraction (XRD) studies of the samples were carried out using a Bruker D8 Advance X-ray diffractometer (40 kV, 40 mA) (Karlsruhe, Germany). Samples were scanned in the range of diffraction angle $2\theta = 1$–$10^\circ$ at a step of 0.01° and a scan speed of 4 s/step. Transmission electron microscopy (TEM) studies were performed using a Philips CM100 electron microscope (Mahwah, NJ) operating at 100 kV.

### 2.4. Film casting

Films were made from ground extrudates by casting. Powders (4%) were dispersed in water and then heated to 95 °C and maintained at that temperature for 10 min, with regular stirring. Subsequently, the suspension was cooled to 65 °C and poured onto petri dishes to make the films. The suspension in petri dishes was dried at 23 °C and 50% relative humidity (RH) for 24 h, after which the films were peeled off for further testing.

### 2.5. Properties of starch–nanoclay composite films

Water vapor permeability (WVP) was determined gravimetrically according to the standard method ASTM E96-00 (ASTM, 2000). All measurements were replicated three times. The films were fixed on top of test cells containing a desiccant (silica gel). Test cells then were placed in a relative humidity chamber with controlled temperature and relative humidity (25 °C and 75% RH). After steady-state conditions were reached, the weight of test cells was measured every 12 h over 3 days. The water vapor transmission rate (WVTR) was determined using Eq. (1):

$$\mathrm{WVTR} = \frac{\left(\frac{G}{t}\right)}{A}\ \mathrm{g/h\ m^2} \tag{1}$$

where $G$, weight change (g); $t$, time (h) and $A$, test area ($m^2$).

WVP was then calculated using Eq. (2):

$$\mathrm{WVP} = \frac{\mathrm{WVTR} \times d}{\Delta p}\ \mathrm{g\ mm/kPa\ h\ m^2} \tag{2}$$

where $d$, film thickness (mm) and $\Delta p$, partial pressure difference across the films (kPa).

Tensile properties of the films were measured using a texture analyzer (TA-XT2, Stable Micro Systems Ltd., UK), based on standard method ASTM D882-02 (ASTM, 2002). All measurements were replicated five times. Films were cut into 1.5 cm wide and 8 cm long strips and conditioned at 23 °C and 50% RH for three days before testing. The crosshead speed was 1 mm/min. Tensile

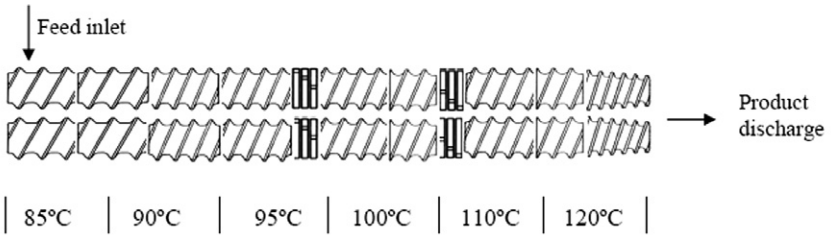


| SE [a,b] | | | | KB[c] | SE | | KB | SE | | |
|---|---|---|---|---|---|---|---|---|---|---|
| 2-30-60 | 2-30-60 | 2-20-60 | 2-15-60 | 4-4-20-30F | 2-15-60 | 2-15-30 | 5-2-20-45R | 2-15-60 | 2-10-30 | 2-10-60 |

[a] SE-Screw elements: double flighted-pitch length (mm)-total element length (mm) (2-30-60).
[b] All screws are forward and intermeshing.
[c] KB-Kneading blocks: number of discs-length of disc (mm)-total element length (mm)-staggering angle of disc-forward (F) or reverse (R) (4-4-20-45 F).

**Fig. 2.** Screw configuration and temperature profile for lab-scale extruder used in the study.

strength (TS) and elongation at break (%E) were calculated using Eqs. (3) and (4):

$$\mathrm{TS} = \frac{L_p}{a} \times 10^{-6}\ \mathrm{MPa} \quad (3)$$

where $L_p$ = peak load (N), and $a$ = cross-sectional area of samples ($m^2$).

$$\%\mathrm{E} = \frac{\Delta l}{l} \times 100 \quad (4)$$

where $\Delta l$ = increase in length at breaking point (mm), and $l$ = original length (mm).

### 2.6. Differential scanning calorimetry

Differential scanning calorimetry (DSC) was used to measure glass transition temperature ($T_g$) of starch–clay nanocomposite films. The test was performed with a Q100 DSC (TA Instruments, New Castle, DE) equipment, fitted with a liquid nitrogen-based cooling system. Samples of the formulated films were first equilibrated at 23 °C and 50% RH for over three days. Then 8–10 mg samples were weighed in aluminium pans and hermetically sealed; an empty pan was used as reference. Each sample was heated from −20 to 120 °C at a heating rate of 10 °C/min. The glass transition temperature ($T_g$) was defined as the midpoint of the transition inflection observed in thermograms. All measurements were performed in triplicates.

### 2.7. Water content

Two grams each of sample films (conditioned as mentioned above) were dried in the oven at 105 °C until constant weight was obtained. Water content can be calculated using Eq. (5):

$$\%\text{water content} = \frac{W_o - W_f}{W_o} \times 100 \quad (5)$$

where $W_o$ was the weight of sample before drying, $W_f$ was the weight of sample after drying. All measurements were performed in triplicates.

### 2.8. Statistical analysis

All the data were analyzed using OriginLab (OriginLab Corporation, Northampton, MA) scientific graphing and statistical analysis software. Statistical significance of differences in means were calculated using the Bonferroni LSD multiple-comparison method at $P < 0.05$.

## 3. Results and discussion

### 3.1. Effects of glycerol content

Fig. 3 shows the effects of glycerol content on XRD patterns of starch–clay nanocomposites. The treatments with 15 and 20% glycerol showed new intensive peaks at lower angles than native MMT. It is generally thought that during the intercalation process the polymer enters the clay galleries and forces apart the platelets, thus increasing the gallery spacing (d-spacing) (McGlashan & Halley, 2003). According to Bragg's law, this would cause a shift of the diffraction peak towards a lower angle. The appearance of the new peak at $2\theta = 4.976°$ (d-spacing = 1.77 nm) with disappearance of the original peak of the nanoclay at $2\theta = 7.210°$ (d-spacing = 1.23 nm) and increase of d-spacing indicated the formation of nanocomposite structure with intercalation of starch chains in the gallery of the silicate layers of MMT. Compared to the two treatments mentioned above, a much wider peak distribution was found for the treatment with 10% glycerol. As for the treatments with 0% and 5% glycerol, further shift of the peaks to smaller angles and even broader peaks were observed. The changes seen in the XRD patterns can be explained by more polymers entering the clay galleries and pushing the platelets further apart. At the first

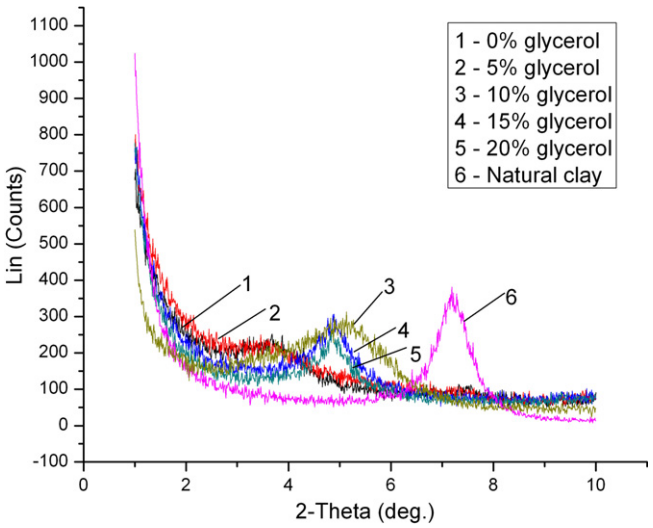


**Fig. 3.** Effects of glycerol content on XRD patterns (1–5: 0–20% glycerol; 6: natural montmorillonite–MMT).

step, the platelets can loose their ordered, crystalline structure and become disordered with the platelets no longer parallel (Dennis et al., 2001). Some clay platelets may even be pushed apart and exfoliated from the stacks of the clay particles. The result is that the XRD peak stays put, but has a broader and wider distribution. At the second step, as more and more polymers enter the galleries, the spacing between clay galleries further increases, leading the XRD peak to continue shifting to the left side. At the same time, more clay platelets are pushed apart by polymers and exfoliated from the stacks of clay particles. As a result, the XRD peak (at the lower angle) becomes wider and wider and finally broadens into the baseline (complete exfoliated nanocomposite structure). For the treatments with 15% and 20% glycerol, most clay platelets were still in ordered, parallel state. At 10% glycerol, platelets lost their ordered structure and were no longer parallel. For 0% and 5% glycerol, large amounts of the clay platelets were exfoliated and randomly distributed in the starch matrix.

The intercalated and exfoliated nanostructure can be confirmed by TEM images. Fig. 4 was representative of TEM images of the starch–clay nanocomposites with 5% and 10% glycerol. In Fig. 4a, more single, disordered clay platelets can be seen, indicating that more exfoliated structures were obtained. While in Fig. 4b, we can see ordered, multilayered nanostructure and some single clay platelets distributing at the edges of the image, meaning lower delamination and dispersion of platelets for the treatments with 10% glycerol.

Similar results were found by Chiou et al. (2007), who compared the effects of 5, 10, and 15 wt% glycerol on clay dispersion. For their samples, adding 5 wt% glycerol produced mostly exfoliated nanoclay, whereas adding 10% or 15% glycerol produced intercalated nanoclay. They concluded that incorporating sufficient glycerol into the starch–nanoclay samples inhibited intercalation to a certain extent because an increase in glycerol–starch interactions might compete with interactions between glycerol, starch, and the clay surface. Pandey and Singh (2005) had examined the effects of the sequence of addition of components (starch/glycerol/clay) on the nature of composites formed. They used 20 wt% glycerol and performed five experiments. They found that when the composites were prepared without earlier plasticization (mixing starch and clay and heating first, then plasticizer), the extent of clay intercalation were increased due to the extensive diffusion of polymer chains inside galleries of clay. They attributed this to two reasons: first, the electrostatic attraction between plasticizer and starch resulted in large structures by developing hydrogen bridges, thus negatively affecting the starch chain mobility; and second, the formation of hydrogen bonds between starch and glycerol decreased the attractive forces between starch and clay. They also compared glycerol/clay and glycerol/starch/clay mixture and found that the glycerol also faced difficulties in moving towards the gallery due to the hydrogen bonding with starch and could not intercalate as freely as in absence of starch. It is also important to note that when nanocomposites are formed by extrusion processing as in the current study, higher specific mechanical energy (SME) input would lead to greater degradation of starch granules leading to increased dispersion of polymer chains within the clay nanolayers. This could be an additional reason for increased degree of exfoliation as plasticizer level decreased from 20% to 5%. The effect of SME on nanocomposite formation was studied separately and the results will be discussed in greater detail in a forthcoming publication.

Fig. 5 shows the effects of glycerol content on WVP. Nanocomposite films with 5% glycerol exhibit the lowest water vapor permeability, indicating that the occurrence of exfoliation was very helpful for improving the barrier properties of the films. At the same time, small amounts of glycerol may facilitate interactions between starch chains and silicate layers of clay and allow glycerol and starch to diffuse together inside the layers of silicates (glycerol will form hydrogen bonds with the starch, replacing the strong interactions between the hydroxyl groups of the starch molecules). That is the reason why samples with 0% glycerol did not show very appreciable WVP performance compared with the 5% glycerol samples, although it also exhibited a partially exfoliated structure. However, with increase in glycerol content beyond 5%, WVP increased because of the decreased extent of clay exfoliation. Fur-

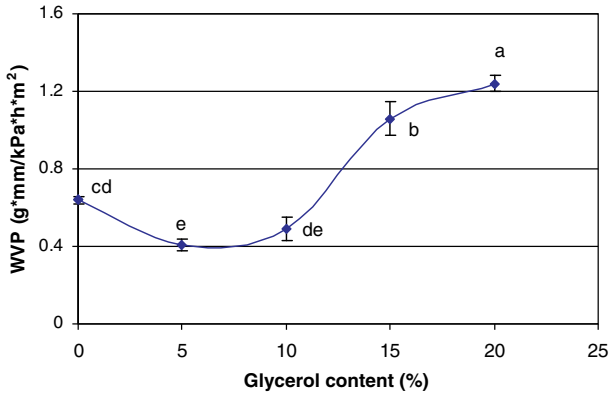


**Fig. 5.** Effect of glycerol content on WVP of corn starch based nanocomposite films with 6% MMT. Error bars indicate the standard deviation. Data points with different letters imply significant difference ($P < 0.05$).

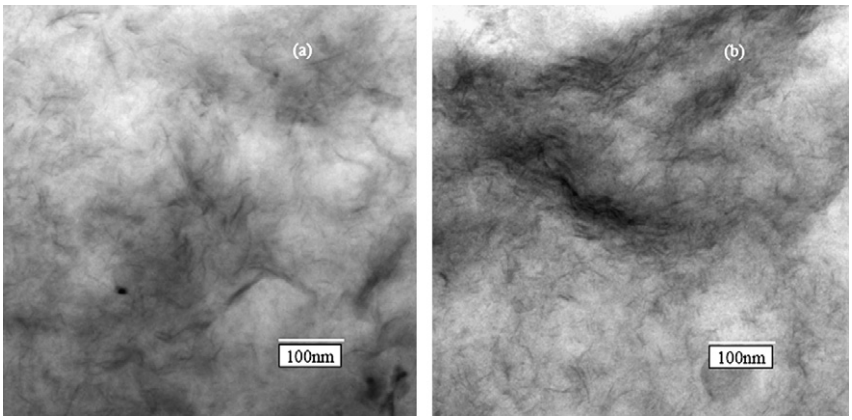


**Fig. 4.** TEM images of starch/clay (6% MMT) nanocomposites with (a) 5% glycerol and (b) 10% glycerol.

thermore, higher glycerol content also increased the hydrophilicity of the starch films. They provided more active sites by exposing hydrophilic hydroxyl groups in which the water molecules could be absorbed (Mali, Grossmann, Garcia, Martino, & Zaritzky, 2006).

Fig. 6 shows the effect of glycerol content on tensile properties. Similar to the WVP results, the film with 5% glycerol had the highest tensile strength due to the formation of exfoliated structure. At the same time, with the increase of glycerol content, the elongation increased. This was because, as a plasticizer, the presence of glycerol facilitates the movement of starch chains, imparting increased film flexibility.

Glass transition temperatures of starch based films were also affected by plasticizer content (Table 1). It has been reported that increasing glycerol content decreases $T_g$ because the polymer matrix becomes less dense and mobility of polymer chains is facilitated with the addition of plasticizer (Mali et al., 2006; McHugh & Krochta, 1994). In Table 1, the $T_g$ of starch based films with different glycerol content displayed almost the same trends as WVP and tensile strength. The films with 5% and 10% glycerol exhibited the highest $T_g$. The results can also be related to the equilibrium water content of the starch based films (Table 1). Lower water content was found for films with 5% and 10% glycerol. Water also exerts a plasticizing effect acting as a mobility enhancer because of its low molecular weight (Mali et al., 2006; Van der Berg, 1991). The formation of exfoliated structure inhibited the absorbance of water molecules into the starch matrix and also inhibited free movement of the starch chains, thus increasing glass transition temperature.

The nanostructure of the polymer/clay hybrids depends on the compatibility and interactions between the base polymer, plasticizers and silicate layers. Due to the strong polar–polar interactions between starch, glycerol and clay surface, a competition mechanism must exist among them. Further studies on the balance of these interactions are needed.

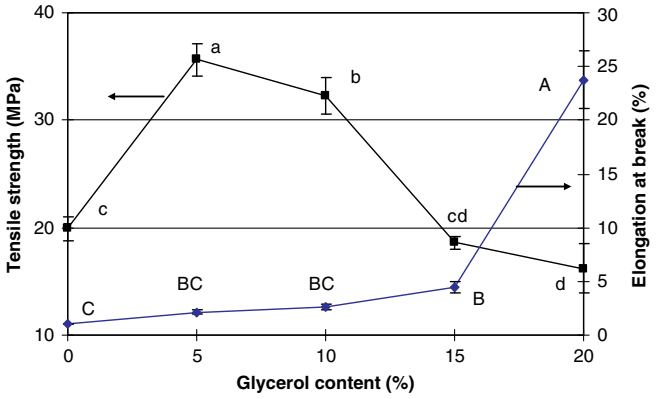


**Fig. 6.** Effect of glycerol content on tensile properties of corn starch based nanocomposite films with 6% MMT. Error bars indicate the standard deviation. Data points with different letters imply significant difference ($P < 0.05$).

**Table 1**
Glass transition temperature ($T_g$) and water content of starch–clay nanocomposite films with different glycerol content

| Glycerol content (%) | Glass transition, $T_g$ (°C) | Water content (%) |
|---|---|---|
| 0 | 52.36 ± 1.90[a] | 11.81 ± 0.12[b,c] |
| 5 | 53.78 ± 4.10[a] | 10.47 ± 0.15[c] |
| 10 | 53.42 ± 2.25[a] | 10.10 ± 0.52[c] |
| 15 | 50.71 ± 2.76[a] | 13.06 ± 1.73[b,c] |
| 20 | 48.97 ± 2.12[a] | 15.03 ± 2.67[b] |

Mean ± standard deviation of each analysis.
Means with the same letters are not significantly different ($P < 0.05$).
Comparisons are made within the same column; $n = 3$ for all treatments.

### 3.2. Effect of different plasticizers

For conventional starch-based films, glycerol is the most commonly used plasticizer. In order to further investigate the role of plasticizers on the formation of nanocomposite structure, two different plasticizers (urea and formamide) with amide groups were selected for the preparation of starch–clay nanocomposites. Glycerol was used as a contrast. Although 5% was the best concentration of glycerol in terms of water vapor permeability and tensile strength, the corresponding elongation was very low, making the film hard to handle because of its brittleness. Considering that elongation and flexibility of films is very important for packaging applications, 15% plasticizer concentration was used for this series of experiments.

Fig. 7 shows the chemical structures of glycerol, urea, and formamide. It is reported that the amide groups in urea and formamide are more advantageous to the formation of hydrogen bonds with starch during the starch thermoplastic process, compared with the hydroxyl groups in glycerol (Ma et al., 2004). Because each urea molecule has two amide groups, it can form more stable hydrogen bonds with starch than formamide. Therefore, the order of the hydrogen bond-forming abilities with starch would be urea > formamide > glycerol.

Fig. 8 shows the XRD patterns of starch–clay nanocomposites based on different plasticizers at 15% level. The treatment with

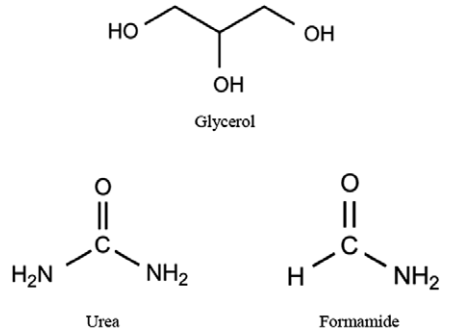


**Fig. 7.** Chemical structures of glycerol, urea, and formamide.

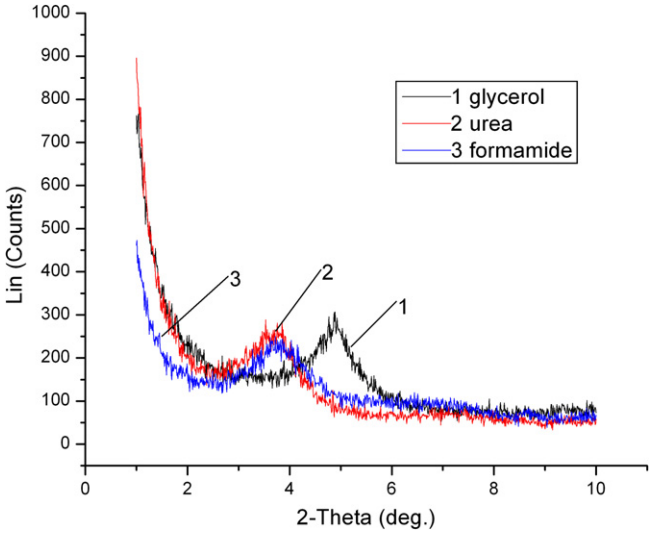


**Fig. 8.** XRD patterns of corn starch–clay nanocomposites with 6% MMT, plasticized using 15% glycerol (1), urea (2), and formamide (3).

glycerol as a plasticizer exhibited a peak at $2\theta = 4.976°$, whereas treatments with both urea and formamide exhibited peaks at $2\theta = 3.860°$. The left shift of the XRD curve indicated that more polymers (and/or plasticizers) entered the clay gallery and the clay platelets were forced further apart.

Fig. 9 shows the WVP of starch–clay nanocomposite films based on different plasticizers. The use of urea and formamide as the plasticizers decreased the WVP of the films as compared to glycerol plasticized films. That meant the new plasticizers (urea and formamide) facilitated stronger interactions between the starch matrix and clay surface. More starch chains entered the clay galleries, leading to the decrease of WVP. In other words, the use of urea and formamide improved the balance of interactions between starch, plasticizer and clay, and allowed more plasticizer and starch to diffuse together inside the layers of silicates. Interestingly, between the three plasticizers WVP of formamide-plasticized films was the lowest. A urea molecule has two amino groups, and it can form more stable hydrogen bonds with starch than can glycerol and formamide, but at the same time it was also the easiest for urea to react with the clay surface. Formamide has intermediate hydrogen bond forming abilities, and it may function as a better bridge between the starch and clay surface, leading to more polymers entering the clay galleries and stronger connections between them.

Table 2 shows the tensile properties of starch–clay nanocomposite films based on different plasticizers. The films based on formamide exhibited the highest tensile strength. However, the films based on glycerol exhibited the highest elongation. Urea is a high melting solid with little internal flexibility, hence urea plasticized nanocomposite films showed the lowest elongation.

Table 3 shows the $T_g$ and water content of starch–clay nanocomposite films plasticized by different plasticizers. Similar to the results of WVP and tensile properties, the films plasticized with formamide exhibited the highest $T_g$ (54.74 °C) and lowest water content (9.75%).

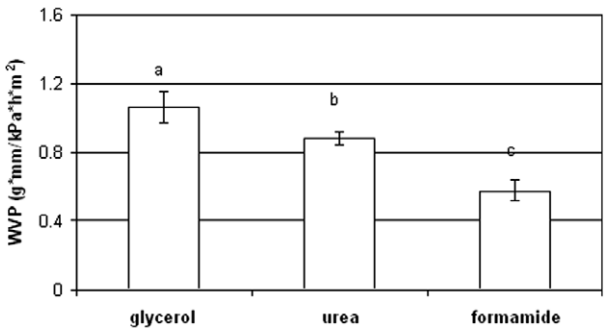


**Fig. 9.** Water vapor permeability (WVP) of corn starch-based nanocomposite films with 6% MMT using different plasticizers at 15% concentration. Error bars indicate the standard deviation. Columns with different letters imply significant difference ($P < 0.05$). WVP of films without any clay using the same base polymer and glycerol level was 1.61 g mm/kPa h m$^2$ (Tang et al., 2008).

**Table 2**
Tensile properties of corn starch-based nanocomposite films with different plasticizers

| | Tensile strength (MPa) | Elongation at break (%) |
|---|---|---|
| Glycerol | 18.60 ± 0.63$^b$ | 4.44 ± 0.52$^c$ |
| Urea | 21.19 ± 2.69$^b$ | 2.49 ± 0.55$^d$ |
| Formamide | 26.64 ± 3.02$^a$ | 3.25 ± 0.59$^d$ |

Mean ± standard deviation of each analysis.
Means with the same letters are not significantly different ($P < 0.05$).
Comparisons are made within the same column; $n = 5$ for all treatments.
Tensile strength and elongation of films without any clay using the same base polymer and glycerol level were 14.22 MPa and 5.26%, respectively (Tang et al., 2008).

**Table 3**
Glass transition temperature ($T_g$) and water content of starch–clay nanocomposite films with different plasticizers

| Plasticizer | Glass transition, $T_g$ (°C) | Water content (%) |
|---|---|---|
| 15% Glycerol | 50.71 ± 2.76$^a$ | 13.06 ± 1.73$^b$ |
| 15% Urea | 53.37 ± 0.79$^a$ | 11.63 ± 0.18$^{bc}$ |
| 15% Formamide | 54.74 ± 1.21$^a$ | 9.75 ± 0.21$^c$ |

Mean ± standard deviation of each analysis.
Means with the same letters are not significantly different ($P < 0.05$).
Comparisons are made within the same column; $n = 3$ for all treatments.

## 4. Conclusions

It was demonstrated in the study that presence of plasticizers greatly affected the formation of nanostructure and barrier, mechanical, and thermal properties of the nanocomposite films. When the glycerol content decreased from 20% to 5%, the degree of clay exfoliation increased. Films with 5% glycerol exhibited the lowest water vapor permeability (0.41 g mm/kPa h m$^2$), highest $T_g$ (53.78 °C), and highest tensile strength (35 MPa), but low elongation at break (2.15%). Urea and formamide were tested as alternative plasticizers for the starch–clay nanocomposites. The results indicated that the use of new plasticizers increased the degree of clay exfoliation. The formamide plasticized starch–clay nanocomposite films exhibited lower water vapor permeability (0.58 g mm/kPa h m$^2$), higher $T_g$ (54.74 °C), and higher tensile strength (26.64 MPa) than the films plasticized with the other two plasticizers when used at the same level (15 wt%). It was concluded that due to the strong polar–polar interactions between starch, plasticizer, and clay surface, the balance of the interactions between them might control the formation of nanocomposite structure and further affect the performance of nanocomposite films.

## Acknowledgements

The authors would like to thank Mr. Eric Maichel, Operations Manager, KSU Extrusion Center, for conducting all extrusion runs. We also would like to thank the KSU milling lab for providing milling facilities. This is Contribution Number 08-126-J from the Kansas Agricultural Experiment Station, Manhattan, Kansas 66506.

## References

ASTM (2000). Standard test methods for water vapor transmission of materials, E96-00. In *Annual book of ASTM standards*, Philadelphia, PA. American Society for Testing and Material.

ASTM (2002). Standard test method for tensile properties of thin plastic sheeting, D882-02. In *Annual book of ASTM standards*, Philadelphia, PA. American Society for Testing and Material.

Avella, M., De Vlieger, J. J., Errico, M. E., Fischer, S., Vacca, P., & Volpe, M. G. (2005). Biodegradable starch/clay nanocomposite films for food packaging applications. *Food Chemistry, 93*, 467–474.

Chiou, B., Wood, D., Yee, E., Imam, S. H., Glenn, G. M., & Orts, W. J. (2007). Extruded starch–nanoclay nanocomposites: Effects of glycerol and nanoclay concentration. *Polymer Engineering and Science, 47*, 1898–1904.

De Carvalho, A. J. F., Curvelo, A. A. S., & Agnelli, J. A. M. (2001). A first insight on composites of thermoplastic starch and Kaolin. *Carbohydrate Polymers, 45*, 189–194.

Dennis, H. R., Hunter, D. L., Chang, D., Kim, S., White, J. L., Cho, J. W., et al. (2001). Effect of melt processing conditions on the extent of exfoliation in organoclay-based nanocomposites. *Polymer, 42*, 9513–9522.

Giannelis, E. P. (1996). Polymer layered silicate nanocomposites. *Advanced Materials, 8*(1), 29–35.

Hulleman, S. H., Janssen, F. H. P., & Feil, H. (1998). The role of water during plasticization of native starches. *Polymer, 39*, 2043–2048.

Kojima, Y., Usuki, A., Kawasumi, M., Okada, A., Fukushima, Y., Kurauchi, T., et al. (1993a). Mechanical properties of nylon 6-clay hybrid. *Journal of Materials Research, 8*, 1185–1189.

Kojima, Y., Usuki, A., Kawasumi, M., Okada, A., Kurauchi, T., & Kamigaito, O. (1993b). Sorption of water in nylon 6-clay hybrid. *Journal of Applied Polymer Science, 49*, 1259–1264.

Kurokawa, Y., Yasuda, H., & Oya, A. (1996). Preparation of a nanocomposite of polypropylene and smectite. *Journal of Materials Science Letters, 15*, 1481–1483.

Ma, X., & Yu, J. G. (2004). The plasticizers containing amide groups for thermoplastic starch. *Carbohydrate Polymers, 57*, 197–203.

Ma, X., Yu, J., & Feng, J. (2004). Urea and formamide as a mixed plasticizer for thermoplastic starch. *Polymer International, 53*, 1780–1785.

Mali, S., Grossmann, M. V. E., Garcia, M. A., Martino, M. N., & Zaritzky, N. E. (2006). Effects of controlled storage on thermal, mechanical and barrier properties of plasticized films from different starch sources. *Journal of Food Engineering, 75*, 453–460.

McGlashan, S. A., & Halley, P. J. (2003). Preparation and characterization of biodegradable starch-based nanocomposite materials. *Polymer International, 52*, 1767–1773.

McHugh, T. H., & Krochta, J. M. (1994). Sorbitol- vs glycerol plasticized whey protein edible films: Integrated oxygen permeability and tensile property evaluation. *Journal of Agricultural and Food Chemistry, 42*, 841–845.

Pandey, J. K., & Singh, R. P. (2005). Green nanocomposites from renewable resources: Effect of plasticizer on the structure and material properties of clay-filled starch. *Starch, 57*, 8–15.

Park, H., Lee, W., Park, C., Cho, W., & Ha, C. (2003). Enviromentally friendly polymer hybrids. Part 1. Mechanical, thermal and barrier properties of thermoplastic starch/clay nanocomposites. *Journal of Materials Science, 38*, 909–915.

Park, H., Li, X., Jin, C., Park, C., Cho, W., & Ha, C. (2002). Preparation and properties of biodegradable thermoplastic starch/clay hybrids. *Macromolecular Materials and Engineering, 287*, 553–558.

Ray, S., Quck, S. W., Easteal, A., & Chen, X. D. (2006). The potential use of polymer–clay nanocomposites in food packaging. *Internation Journal of Food Engineering, 2*(4), Art 5.

Sinha Ray, S., Maiti, P., Okamoto, M., Yamada, K., & Ueda, K. (2002). New polylactide/layered silicate nanocomposites. 1. Preparation, characterization and properties. *Macromolecules, 35*, 3104–3110.

Sinha Ray, S., & Okamoto, M. (2003). Polymer/layered silicate nanocomposites: A review from preparation to processing. *Progress in Polymer Science, 28*, 1539–1641.

Sinha Ray, S., Yamada, K., Okamoto, M., & Ueda, K. (2002). New polylactide/layered silicate nanocomposite: A novel biodegradable material. *Nano Letters, 2*, 1093–1096.

Sorrentino, A., Gorrasi, G., & Vittoria, V. (2007). Potential perspective of bio-nanocomposites for food packaging applications. *Trends in Food Science & Technology, 18*, 84–95.

Tang, X. Z., Alavi, S., & Herald, T. J. (2008). Barrier and mechanical properties of starch-clay nanocomposite films. *Cereal Chemistry, 85*(3), 433–439.

Usuki, A., Kato, M., Okada, A., & Kurauchi, T. (1997). Synthesis of polypropylene-clay hybrid. *Journal of Applied Polymer Science, 63*, 137–139.

Vaia, R. A., & Giannelis, E. P. (1997). Polymer melt intercalation in organically-modified layered silicates: Model predictions and experiment. *Macromolecules, 30*, 8000–8009.

Vaia, R. A., Jandt, K. D., Kramer, E. J., & Giannelis, E. P. (1995). Kinetics of polymer melt intercalation. *Macromolecules, 28*, 8080–8085.

Van der Berg, C. (1991). Food water relationships: Progress and integration, comments and thoughts. In H. Levine & L. Slade (Eds.), *Water relationships in foods* (pp. 21–28). New York: Plenum Press.

Wilhelm, H. M., Sierakowski, M. R., Souza, G. P., & Wypych, F. (2003). Starch films reinforced with mineral clay. *Carbohydrate Polymers, 52*, 101–110.